Location and spatial shape of electron beams in Io's wake

S. Jacobsen,[1] J. Saur,[1] F. M. Neubauer,[1] B. Bonfond,[2] J.-C. Gérard,[2] and D. Grodent[2]

[1] The Galileo spacecraft observed energetic field-aligned electron beams very close to Io during several flybys. We apply a three-dimensional magnetohydrodynamic (MHD) model of the far-field Io-Jupiter interaction to simulate for the first time the location and spatial shape of field-aligned electron beams. Io continuously generates MHD waves by disturbing the Jovian magnetoplasm. Currents carried by Alfvén waves propagate predominantly along the magnetic field lines. As the number of charge carriers decreases along the travel path, electrons are accelerated toward Jupiter. These energetic electrons precipitate into the Jovian ionosphere, visible as prominent Io footprint emission. Electrons are also accelerated toward Io and form the equatorial beams observed by the Galileo spacecraft. Unlike the beam formation, the position and spatial structure of these beams have not been addressed in detail before. We use a 3-D MHD model with initial conditions corresponding to the individual Galileo flyby and determine the spatial morphology of the beams in Io's orbital plane. Our results for the beam locations are in good agreement with the Galileo Energetic Particle Detector observations. We find that the ratio of the one-way travel time of the Alfvén wave from Io to Jupiter and the convection time of the plasma past the obstacle controls the location of the beam. This leads to the conclusion that at other satellites with other plasma environments, the electrons might not be close to the satellite but can be shifted significantly downstream along its plasma wake. Thus, the future search for electron beams near a satellite should be further extended to the wake region.

1. Introduction

[2] Io's powerful interaction with the surrounding plasma generates auroral footprints in Jupiter's atmosphere with an input power of up to 100 GW [*Clarke et al.*, 1996; *Prangé et al.*, 1996]. The auroral footprints were first observed by *Connerney et al.* [1993] and are assumed to be generated by energetic electrons which are accelerated downward (planetward) and precipitate into Jupiter's upper atmosphere [*Dols et al.*, 2000; *Gérard et al.*, 2006]. Throughout this paper, we will use the terms "downward" in the sense of "planetward" and "upward" in the sense of "antiplanetward." Whenever the terms upward or downward are used in the context of electron beams, we mean the direction of electron acceleration. Associated with Io's interaction, energetic field-aligned electron populations have also been observed in situ by the Galileo spacecraft near Io. *Williams et al.* [1996, 1999] and *Frank and Paterson* [1999] report

intense bidirectional electron beams in Io's wake and *Williams and Thorne* [2003] observe high-energy electrons streaming onto Io's poles during two polar flybys (I31, I32). The measured pitch angle distributions suggest that these electron beams originate at high latitudes close to Jupiter where electrons are accelerated upward (antiplanetward) toward Io. Even though the exact link between the planetward and antiplanetward electron beams at Io is not fully understood, the process of antiplanetward electron beams in association with auroral features appears to be a universal property of aurorae [*Saur et al.*, 2006]. These beams are known to occur close to Io, in the magnetosphere of the Earth [*Klumpar*, 1990; *Carlson et al.*, 1998], Jupiter [*Tomás et al.*, 2004; *Frank and Paterson*, 2002a; *Mauk and Saur*, 2007] and Saturn [*Saur et al.*, 2006; *Mitchell et al.*, 2009]. A main advantage in studying Io's auroral footprints and energetic particle populations compared to other solar system auroral features is that the location of the initial source region, i.e., Io's interaction region, is known and the perturbation is continuous.

[3] Io is embedded in a dense plasma torus centered around the centrifugal equator which is tilted with respect to Io's orbital plane. As Io moves up and down in the torus on its orbit, it continuously generates MHD waves by disturb-

[1]Institut für Geophysik und Meteorologie, Universität zu Köln, Cologne, Germany.
[2]Laboratory for Planetary and Atmospheric Physics, Université de Liège, Liège, Belgium.
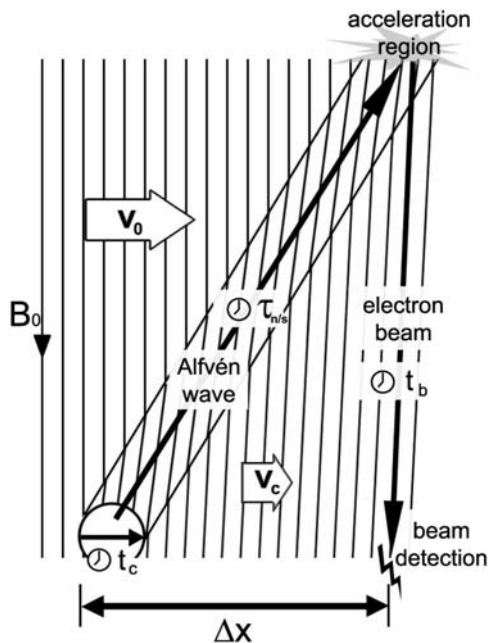
Figure 1. Sketch of the processes and time scales starting from the Alfvén wave generation to the beam detection by a spacecraft. The Alfvén wing continues upward, after a small fraction of its energy is diverted into electron beam heating. The thick black arrows show the directions of corotation, Alfvén wave and beam propagation in Io's rest frame; clock symbols depict the related characteristic times we refer to. Dimensions and angles are not to scale.

ing the incoming plasma of varying density. Electric currents are carried predominantly by Alfvén waves that propagate along the magnetic field in the rest frame of the plasma. In Io's rest frame these waves form a wing-like structure called Alfvén wing [*Drell et al.*, 1965]. They are partly reflected at density gradients such as the plasma torus boundary. The reflection process and geometry are strongly depending on the incoming plasma density at Io and thus on Io's position in the torus. Due to irregular reflection angles and interference phenomena this has a significant impact on the Io footprint morphology, especially on the shape and spacing between secondary spots observed in the trail feature [*Gérard et al.*, 2006; *Bonfond et al.*, 2009]. A more detailed study of this interrelationship has been published by *Jacobsen et al.* [2007].

[4] Outside the plasma torus the number of charge carriers decreases rapidly, whereas the magnetic field strength increases and the cross section of the current channeling flux tubes becomes smaller. To maintain the current flow, the electrons must be accelerated. It happens where the ion density decreases below a certain threshold value [*Knight*, 1973] in the region where the maximum Alfvén velocity is reached [*Su et al.*, 2003]. This acceleration triggers short-burst radio emissions near 20 MHz [*Zarka*, 1998]. The acceleration region is located between an altitude of approximately 0.9 R_J and 2.9 R_J [*Hess et al.*, 2007]. The acceleration mechanism has been widely discussed and is still under debate. Concepts like electrostatic double layers [*Smith and Goertz*, 1978], kinetic or inertial Alfvén waves [*Swift*, 2007; *Jones and Su*, 2008] and repeated Fermi

accelerations [*Crary*, 1997] have been brought up and modeled. It has mostly been done to interpret the planetward beams as a source for the aurora. For Earth, *Mauk et al.* [2002] distinguish between three types of aurora: (1) Alfvén aurora and aurora associated with (2) upward and (3) downward current regions. For Jupiter, *Su et al.* [2003] follow this argumentation and identify the main spot emission as Alfvén aurora.

[5] The electron beams at Jupiter have first been observed near the equator with the Energetic Particle Detector (EPD) on the Galileo spacecraft. In December 1995, during the first Io flyby an energetic field-aligned electron population was measured in Io's wake [*Williams et al.*, 1996]. The pitch angle distribution was bidirectional. In 2001 two polar flybys took place. I31 (northern pass) and I32 (southern pass) both showed energetic electrons streaming onto Io's polar caps [*Williams and Thorne*, 2003] and bidirectional beams in the wake region. The authors present the flux and pitch angle distribution of electrons with energies of 15 to 93 keV. The number of electrons with a pitch angle near 0° and 180° exceeds the counts of electrons around 90° by a factor of ten. The spectral distribution of electrons with energies of 15 to 188 keV reveals a power law decrease in the flux with higher energies [*Williams et al.*, 1999]. Further evidence for the existence of cross-hemisphere electron beams arises from Hubble Space Telescope (HST) observations of the Jovian aurora. A leading spot that precedes the Io footprint in the Jovian aurora has been reported by *Bonfond et al.* [2008]. In their publication, they propose a cross-hemisphere electron beam to trigger an auroral emission in the conjugate hemisphere. This might be either a leading spot or a secondary spot feature depending on Io's position in the torus. *Saur et al.* [2002] and *Dols et al.* [2008] have shown that precipitating electrons with energies between 0.1 and several keV contribute significantly to the formation of Io's ionosphere. Thus, investigation of these electron beams is also important because in models of the local interaction, the spatial distribution of the ionization rate owing to the energetic electrons is only poorly constrained and future models will benefit from improved constraints.

[6] Our aim is to study the spatial distribution and locations of the antiplanetward electron beams near Io. Besides Io, there are other satellites, that interact similarly with a planetary magnetosphere, for example Ganymede, Callisto, Europa and Enceladus. The principle results of our work might be applicable to those satellites as well. The topic of electron beam generation/acceleration mechanism is beyond the scope of this paper.

2. General Considerations

[7] The Alfvén wave generated by Io follows the Alfvén characteristic toward Jupiter [*Neubauer*, 1980]. In Io's rest frame the propagation direction is tilted with respect to the background magnetic field by the Alfvén angle $\Theta_A = \arctan(M_A)$, with the Alfvénic Mach number M_A. The time required to reach the acceleration region in the northern (*n*) or southern (*s*) hemisphere is called one-way travel time $\tau_{n/s}$ (Figure 1). During this time the magnetic field line that carries the Alfvén wave is convected with the moving plasma. The longer the traveltime, the further downstream

Table 1. Parameters Used in Our MHD Simulations

Flyby	System III Longitude (deg)	Centrifugal Latitude (deg)	Local Electron Density n_e (cm^{-3})	Local Mass Density ρ (amu cm^{-3})	Travel Time North $\tau_{n,1/2}$ (s)	Travel Time South $\tau_{s,1/2}$ (s)
I0	80.1	1.917	2142	36250	305	470
I31	159.4	4.867	1853	31360	185	537
I32	260.2	3.192	2043	34580	262	516

it reaches the acceleration region. We call the three-dimensional region, where the particle acceleration takes place and which is fed by the Alfvén wave energy, the volume of beam generation. Once an upward beam has formed in this volume, it follows the magnetic field line and passes the equatorial plane after the beam traveltime t_b. Like the downstream shift of the beam generation volume, the downstream offset of the location where the beam penetrates the equatorial plane of Io grows due to field line convection with the combination of the one-way traveltime and the beam traveltime $\tau_{n/s} + t_b$.

[8] Another element that has to be taken into account is the magnetic field direction. The locus of a field-aligned beam is given by the magnetic field topology it tends to follow. The magnetic field is perturbed and draped around Io due to the electromagnetic interaction. This draping is accompanied by a deceleration of the plasma. The convection time t_c, i.e., the time a plasma particle needs to cover the interaction distance of one Io diameter, becomes larger, the stronger the interaction. Thus the downstream offset is inversely proportional to the interaction strength. Accordingly, a simple relation for the downstream offset $\Delta x_{n/s}$ of electron beams from the north (n) and south (s) is

$$\Delta x_{n/s} = \int_{0}^{\tau_{n/s}+t_{b,n/s}} v_c \, dt \qquad (1)$$

[9] For the decelerated plasma at constant convection speed $v_c = 2R_{Io}/t_c$ this relation can be rewritten as a first-order approximation as

$$\frac{\Delta x_{n/s}}{2R_{Io}} = \frac{\tau_{n/s} + t_{b,n/s}}{t_c} \qquad (2)$$

[10] The traveltimes $\tau_{n/s}$ are strongly coupled to Io's position in the torus which varies with system III longitude (Table 1) [*Bagenal*, 1983]. The convection time depends on the incoming plasma density. The denser the plasma, the stronger the interaction, i.e., the deceleration of the plasma and the longer the convection time. As the torus plasma density is a function of centrifugal latitude, the convection time is also coupled to Io's position in the torus, i.e., also to system III longitude. Hence, following equation (2), we expect the downstream offset of an electron beam at Io to vary with its orbital position. However, the local convection speed is not uniform but varies along a streamline in the vicinity of Io. Therefore it is necessary to model the plasma bulk velocity field and the magnetic field consistently to obtain reliable results. Furthermore the shape and morphology of the Io footprint in the Jovian aurora changes when Io moves within the torus [*Bonfond et al.*, 2008]. If the downward electron beams develop a complicated pattern it

is likely that upward beams are also affected in this way. *Jacobsen et al.* [2007] have shown that nonlinear wave reflection processes significantly contribute to the variation of the footprint morphology. Therefore reflection processes at plasma density gradients have to be taken into account. Historically, the interaction of Io with the Jovian magnetosphere has been first described as unipolar inductor by *Goldreich and Lynden-Bell* [1969]. In this framework, the travel time of the Alfvén wave is small compared to the convection time ($\tau/t_c \ll 1$). An upward electron beam in such an environment would hit Io and cover almost the whole area of the initial interaction. With the discovery of the Io plasma torus, it became clear that the high plasma density would lead to a substantially smaller Alfvén velocity than previously expected. *Neubauer* [1980] developed the ideal Alfvén wing model to describe the Io interaction. Using these assumptions the ratio of Alfvénic traveltime and convection time becomes much larger ($\tau/t_c \gg 1$). Galileo observations of the plasma bulk velocity near Io exhibit a remarkable deceleration of the plasma [*Frank and Paterson*, 2002b]. Consequently, the convection time is of the same order as the Alfvénic travel time ($\tau/t_c \approx 1$). In this sense the Io interaction represents an intermediate scenario, between the two extreme cases specified in the "unipolar inductor model" and the "ideal Alfvén wing model."

[11] Although discussion of the beam generation mechanism is beyond the scope of this publication, we require a geometric concept of the beam generation volume for our studies. Although upward accelerated electrons are generally associated with downward current regions in the aurora, observations by *Klumpar et al.* [1988] and *Carlson et al.* [1998] for the Earth's aurora have shown that this attribution is not unambiguous [*Mauk et al.*, 2002]. Parallel electric fields associated with the two branches of the current system are believed to accelerate the electrons in both directions. Phase space density (PSD) spectra of the observed particles provide hints for the acceleration mechanism. Electron beams generated by parallel electric fields show remnants of a coherent acceleration in the form of a peak in PSD for a certain energy [*Mauk et al.*, 2001]. *Swift* [2007] has demonstrated that field aligned electron acceleration by inertial Alfvén waves produces upward beams with a broad energy distribution without a PSD peak. In contrast to these strictly field-aligned acceleration mechanisms, a stochastic process (reminiscent of heating) can contribute significantly to the electron acceleration. For Jupiter this has been discussed by *Frank and Paterson* [2002a]. *Williams et al.* [1999] have shown that the PSD spectra of the beams observed by Galileo do not exhibit a significant peak but decrease monotonically with energy and follow a power law.

[12] The Io-generated currents are generally directed upward (toward Io) on the Jupiter-facing side and downward (to Jupiter) on the opposite side. There is a current reversing layer between the two branches (Figure 2b). In
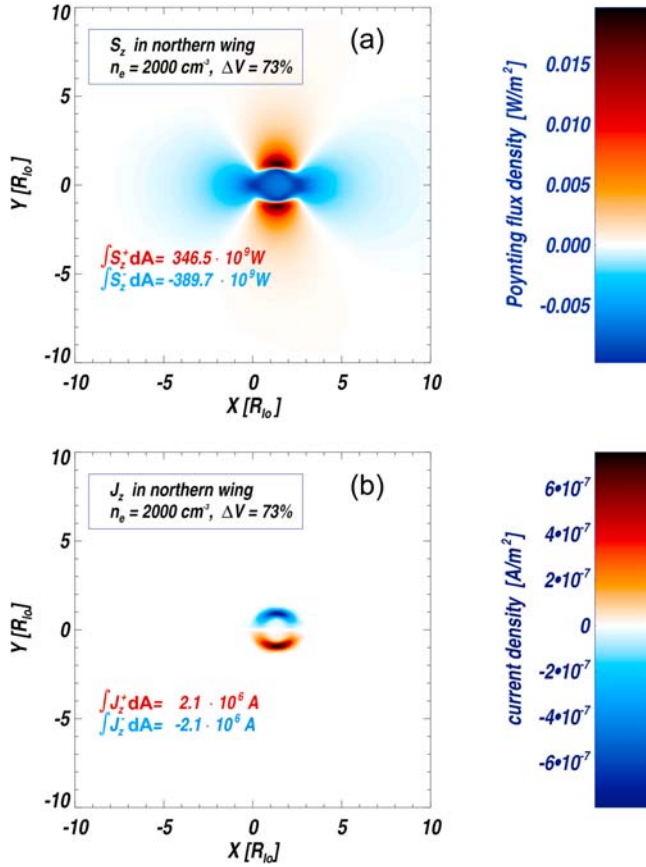
Figure 2. Different topology of z components of (a) Poynting flux density S_z and (b) current density j_z in the northern Alfvén wing at a distance of z = 5 R_{Io} above Io's pole.

case of a distinct association of the beam with a predominant current direction toward or away from Jupiter, equatorial beams should be more likely to be detected on the anti-Jovian side. Galileo EPD observations are not consistent with this picture. For the I0 flyby the radial profile of Io's wake does not show any hint for an asymmetry between the Jovian and anti-Jovian part of the wake [*Williams et al.*, 1999]. Unfortunately the instrument performed a background scan just during the passage of the current reversing layer. In contrast, the I31 trajectory is almost entirely in the current reversing layer area of the Io current system and EPD data exhibits intense beams. Finally, I32 does not feature a significant variation in the beam intensity as one would expect from the trajectory that covers the current reversing layer and the maximum downward current area. It is noteworthy that a strong filamentation of Io's current system has been discussed [*Chust et al.*, 2005]. These highly structured currents would result in a more symmetric current-associated beam distribution over the poles. Still, the measured PSD spectra lack a peak representative for current system associated acceleration.

[13] The criteria derived from Galileo EPD data favor an acceleration mechanism for the antiplanetward acceleration, which is reminiscent in its features of heating. The broad energy distribution reported by *Williams and Thorne* [2003]

is consistent with electron acceleration by inertial Alfvén waves [*Swift*, 2007] and the upward acceleration mechanism appears to be distributed within both, the sub-Jovian and the anti-Jovian side of Io's Alfvén wings.

[14] Io's Alfvén wings communicate electromagnetic energy between Jupiter and Io. This energy balance is described by Poynting's theorem

$$\iint \mathbf{S} \, d\mathbf{A} = -\iiint \mathbf{j} \cdot \mathbf{E} \, dV \qquad (3)$$

[15] With the Poynting flux density $\mathbf{S} = (\mathbf{E} \times \mathbf{B})/\mu_0$, an arbitrary Volume V with the surface $\mathbf{A}$, electric field $\mathbf{E}$ and the permeability of vacuum μ_0. Using $\mathbf{E} + \mathbf{v} \times \mathbf{B} = 0$, we can write

$$\iint \mathbf{S} \, d\mathbf{A} = \iiint \mathbf{j} \cdot (\mathbf{v} \times \mathbf{B}) dV \qquad (4)$$

and finally

$$\iint \mathbf{S} \, d\mathbf{A} = \iiint -\mathbf{v} \cdot (\mathbf{j} \times \mathbf{B}) dV \qquad (5)$$

[16] The energy needed for the electron acceleration is a fraction of the energy which is being communicated between Io and Jupiter. This energy becomes available by the work done by the $\mathbf{j} \times \mathbf{B}$ force which slows down the corotating plasma in the Jovian ionosphere. From equation (5) we can see that the Poynting flux density can be used to calculate the energy flux.

[17] Interestingly, the direction of the Poynting flux density depends on the rest frame under consideration. In the rotating system of Jupiter, we find $\mathbf{E} \cdot \mathbf{j} > 0$ in the Jovian ionosphere and $\mathbf{E} \cdot \mathbf{j} < 0$ at Io. This condition means that in this frame Jupiter represents a load whereas Io serves as a generator (see *Mauk et al.* [2002] for a detailed discussion). The Poynting flux density in the Alfvén wing is directed toward Jupiter. In Io's rest frame, this interrelation is reversed. Io represents the load ($\mathbf{E} \cdot \mathbf{j} > 0$) in this system and the Jovian ionosphere acts as the generator. The Poynting flux density is directed toward Io. For an isolated view of the Io-Jupiter interaction with no other sources and sinks for energy than Io and the Jovian ionosphere, the energy $\Delta\varepsilon$ that is dissipated in a volume that contains the load is given by the Poynting flux through the surface $\mathbf{A}_s$ perpendicular to the background magnetic field $\mathbf{B}_0$ between generator and load. For our simulation, where $\mathbf{B}_0 \parallel -z$, this is given by

$$\Delta\varepsilon = \iint \mathbf{S}|_z \, d\mathbf{A}_s \qquad (6)$$

where

$$\mathbf{S}|_z = \frac{1}{\mu_0}(\mathbf{E} \times \mathbf{B})|_z = \mathbf{v}_\perp|_z \frac{B^2}{\mu_0} \qquad (7)$$

and $d\mathbf{A}_s \parallel \mathbf{B}_0$.

[18] Altogether, the Poynting flux describes the energy transport to the acceleration region and it matches the morphological requirements derived from the EPD data. We

therefore use the normalized Poynting flux density as a proxy parameter for the intensity of generated beam.

3. Model and Numerical Method

[19] Our model uses the framework of MHD to describe the Io interaction in the rest frame of the moon. We use the following set of equations:

$$\frac{\partial \rho}{\partial t} + \nabla \cdot (\rho \mathbf{v}) = 0 \tag{8}$$

$$\rho \left(\frac{\partial \mathbf{v}}{\partial t} + \mathbf{v} \cdot \nabla \mathbf{v} \right) = -\nabla p + \frac{1}{\mu_0} (\nabla \times \mathbf{B}) \times \mathbf{B} - \rho \eta \mathbf{v} \tag{9}$$

$$\frac{\partial \mathbf{B}}{\partial t} = \nabla \times (\mathbf{v} \times \mathbf{B}) \tag{10}$$

$$\frac{\partial e}{\partial t} + \nabla \cdot (e\mathbf{v}) = -p \nabla \cdot \mathbf{v} + \frac{\eta}{2} \left(\rho \mathbf{v}^2 + e_n - e \right). \tag{11}$$

[20] We implemented an effective collision frequency η into the equation of motion (equation (9)) and the energy equation (equation (11)). This allows us to locally define an obstacle which acts as an MHD wave generator. We would like to point out that the focus of this study is not to model the near-field interaction of Io in a realistic way, but to use our far-field results to investigate the issue of electron beams. The numerical realization is based on the Zeus-3D MHD code [Stone and Norman, 1992]. It is a time-dependent finite difference code which solves the equations of ideal, single-fluid magnetohydrodynamics with our extensions regarding collisions. For further details, see Jacobsen et al. [2007]. Owing to computing capacity limitations we apply a simplified magnetospheric model. We use a spatially constant background magnetic field and straight field lines antiparallel to the z direction in the initial and upstream conditions. The plasma flow is in x direction, and the y axis completes the right handed coordinate system. As the plasma density varies significantly along a magnetic field line, we include three different plasma regimes in our simulation box: The dense torus plasma, the low-density high-latitude plasma and the Jovian ionosphere. We use a constant value for the torus plasma density and another one for the low-density plasma. The transition between these regimes is linear. The northern and southern Jovian ionosphere is located at the top and the bottom of the simulation box, respectively. Both are represented as a steep linear increase in the plasma density near the edge of the simulation grid. There are no density gradients in the x and y directions in the initial conditions [Jacobsen et al., 2007]. To simulate the Galileo flyby scenarios, we follow Bagenal and Sullivan [1981] and Bagenal [1983] and use their results for a consistent set of the most important boundary and initial conditions for our simulations derived in section 2: traveltime and incident plasma density which controls the convection speed. We use their torus model to determine the incoming plasma density on Io's orbit for the given centrifugal latitude during a flyby. Second, we choose Io's position in the torus such that the one-way Alfvénic travel times in our model

(northward and southward) match the ones from Bagenal [1983]. They are given in Table 1. Io is treated as a spherical cloud of neutral gas represented by the effective collision frequency η in extra terms incorporated into the MHD equations (equations (8) to (11)). Its value is assumed to be constant for $r < 1 \, R_{Io}$ and decreases with a scale height of 100 km for $r > 1 \, R_{Io}$. We determine η so that the simulated minimum plasma convection speed for the I31 scenario meets the observations of 5 km s[1] during this flyby [Williams and Thorne, 2003; Frank and Paterson, 2002b]. We retain this value for η for all simulations. Thus the strength of the plasma interaction is only controlled by the density of the incoming plasma.

[21] Our model calculates plasma parameters such as density, temperature and internal energy as well as bulk velocity, magnetic field and electric currents. We determine the location and intensity of the equatorial electron beams in a two step method. First we determine the Poynting flux in the acceleration region just above the Jovian ionosphere (i.e., the S_z component in our model). We consider this parameter as representative for the generated beam intensity. Then we map this electron beam intensity distribution along the simulated magnetic field lines to x-y plane that contains Galileo's point of closest approach and in a next step further to the opposite ionosphere. With this method we neglect the traveltime of the beam electrons. For energetic electrons as measured by Galileo within the energy range $E = 15$–93 keV it can be approximated by $t_b = l \cdot (2E/m_e)^{-1/2}$ where l is the distance along the magnetic field line from the acceleration region to Io, E is the electron energy and m_e the electron mass. With a mean length of $l = 7 \, R_J$, the value for t_b is below 10 s for electrons with energies >15 keV measured by the EPD instrument and thus it is small compared to the other time scales depicted in Table 1. We therefore neglect the traveltime of the beam. We also do not include drifts off the field lines. We estimate the magnetic gradient and curvature drift using equation (2a) from [Mauk et al., 1999]. For beams with energies of tens of keV and 10 s traveltime the drift is <1 km and the effect can therefore be neglected in our studies.

4. Results

[22] In Figure 2 we show modeled electromagnetic energy flux (Figure 2a) and current density (Figure 2b) for a torus electron density of 2000 cm^{-3}, which is the mean value of the innermost I0 and outermost I31 scenario (Table 1) with respect to the torus center. The total of the simulated currents in one direction is 2.1×10^6 A (Figure 2b). This is in good agreement with observations of 2.6×10^6 A [Acuña et al., 1981] and a value of 3.0×10^6 A calculated with the analytical expression $J = 4\Sigma_A E(R_{io} + H)$ [Neubauer, 1998; Saur, 2004] for the maximum possible current, where Σ_A is the Alfvén conductivity and H is the assumed extension of Io's atmosphere. Model results by Saur et al. [1999] indicate stronger currents of 5×10^6 A. However, these results were obtained for a significantly higher electron density of $n_e = 3600$ cm^{-3} and thus for stronger interaction. Although the current system balance is not the focus of this work, the results provide another confirmation that the parameters chosen for the Io interaction are adequate.

[23] In Io's rest frame the integrated Poynting flux in each direction lies with $\sim 4 \cdot 10^{11}$ W (Figure 2a) in the range of estimated energy flux values collected in the review by *Saur et al.* [2004] of $\sim 10^{12}$ W. Simulation data for the I31 scenario is shown in Figure 3. It illustrates our method of acquiring the equatorial beam topology and the leading-spot offset. Figure 3 (top) shows the Poynting flux density in a x-y plane perpendicular to the background magnetic field above the Jovian ionosphere. The distance from Io is chosen such that the time after which the Alfvén wave reaches this plane is consistent with the actual location of the acceleration region. As argued in section 2, we consider the Poynting flux as a proxy parameter for the electron acceleration. In this sense, Figure 3 (top) shows also the area of beam generation. The stretched, elongated shape is characteristic for various reflection processes under strong interaction conditions [*Jacobsen et al.*, 2007]. As the plasma density gradient in our model is idealized compared to common torus models, the reflection properties do not necessarily match exactly the real reflection behavior. *Jacobsen et al.* [2007] have shown that the model qualitatively reproduces the footprint morphology, nevertheless. Consequently, the effects on the beam shape resulting from reflections should only be interpreted qualitatively. These effects include an elongation in the downstream direction and necking. However, the location of the beam onset is not affected by reflections. Figure 3 (middle) illustrates the x component of the plasma velocity field (color-coded) and the magnetic field lines (solid lines). The transition areas between the plasma regimes are marked by horizontal dash-dotted lines. Reflections at these boundaries are visible in the plasma x velocity data. During reflection the perturbations in **v** and **B** reverse sign depending on the plasma gradient met [*Wright*, 1987]. The supercorotational areas (red) in the downstream region, for instance, are caused by Alfvén waves which are reflected back from the Jovian ionosphere. A reflection at this positive plasma density gradient reverses the sign of the velocity perturbation. The numerous reflections in our simulation interfere and superimpose, finally leading to the complicated alternating structure of decelerated (blue) and accelerated (red) plasma with respect to the background bulk velocity (white). A more detailed discussion of the reflection pattern is given by *Jacobsen et al.* [2007]. We map the Poynting flux structure from the northern acceleration region where the antiplanetward electron beams are generated along the magnetic field lines (Figure 3, middle) to Galileo's orbital plane (Figure 4) and further to the southern ionosphere (Figure 3, bottom). As we do not know the beam generation mechanism in detail it is hard to define a threshold energy for the beam generation. Because of lack of this information, we arbitrarily use 50% of the maximum Poynting flux and mark the spot most upstream where this value is reached by a green star in Figure 3 (top). A beam generated at this position would follow the green field line in Figure 3 (middle) and produce a spot in southern aurora preceding the main spot by 2°–3° (green star in Figure 3 (bottom)). This value is within the range expected from *Bonfond et al.* [2008] who report an observed maximum value of 3.1°.

[24] Figure 4 shows the simulated beam intensity in the flyby plane of Galileo. It includes the spacecraft trajectory. The yellow box denotes the area where field-aligned electron beams have been observed [*Williams and Thorne*, 2003]. Hatched areas depict observed beams from the north and south on the left and right side, respectively. For I0 the agreement is very good for the beam from the north. Especially the necking of the beam compared to the size of the source region is well reproduced. The northward beam shows the same property but is less intense. However, due to mirroring of the beams and small electron travel times, the observed beams are most likely bidirectional unless one direction is shielded by the moons disk. Thus we can interpret the topology of the simulated beams outside Io's disk as bidirectional. The I31 simulations are also consistent with the observations. Although the simulated beam onset is shifted downstream a closer look at the EPD data reveals an increase in the beam intensity [*Williams and Thorne*, 2003]. The measured maximum intensity coincides with the simulated beam onset. Our simulation suggests a continuous beam structure further downstream which cannot be verified by the observations as the pitch angle sampling mode during this flyby yielded information for the beam pitch angles only every 140s. Furthermore the strong overlaying "pancake" distribution in that area might hide weaker beams. A possible interpretation from the simulation point of view could be a stronger necking of the beam as featured by the I32 data. For a beam topology similar to the one simulated with the I32 scenario, the Galileo I31 trajectory might lie outside the beam area that is confined to the wake center. Consistent with our simulation, no beam from the south has been observed as it was shielded by the moon during this northern polar flyby. However, the I31 flyby data does not clearly show evidence for electron beams at the location where I0 data exhibits intense beams in Io's wake region. This fact supports our hypothesis that the location of the equatorial electron beams varies with Io's position in the torus. The I32 scenario of a southern polar flyby is again well reproduced for the northern beam. At the point where the spacecraft appears behind the disk the beam from the north is observed. Our simulation data also exhibit a northern beam at that position. The southern beam cannot be found in our simulation data at the location it was observed.

[25] Overall the beam onset is systematically further downstream in our simulations than measured. We provide three possible interpretations. First the Alfvén travel time could be overestimated. A steeper plasma density gradient at the torus edges as proposed by [*Moncuquet et al.*, 2002] would result in a considerably shorter travel time and thus an upstream shift of the beam location near Io. Furthermore it would yield a smaller north-south asymmetry for the simulated beams. Another interpretation involves the near-Io interaction. The size and shape of Io's ionosphere is probably more extended and structured than implemented in our model and local effects increase the amplitude of the magnetic field perturbation compared to our far-field approach. Simulations of the local interaction details as carried out by *Saur et al.* [2002] provide a value of $\delta B_x \sim 750$ nT for a generic polar flyby. Finally, we only scale the initial Alfvénic perturbation with the incoming plasma density taken from an empirical torus density model. This method neglects transient events like eruptions on Io that might alter Io's interaction with the magnetosphere significantly. The hypothetical possibility of stronger interaction is supported by spacecraft data. The I32 flyby magnetic field
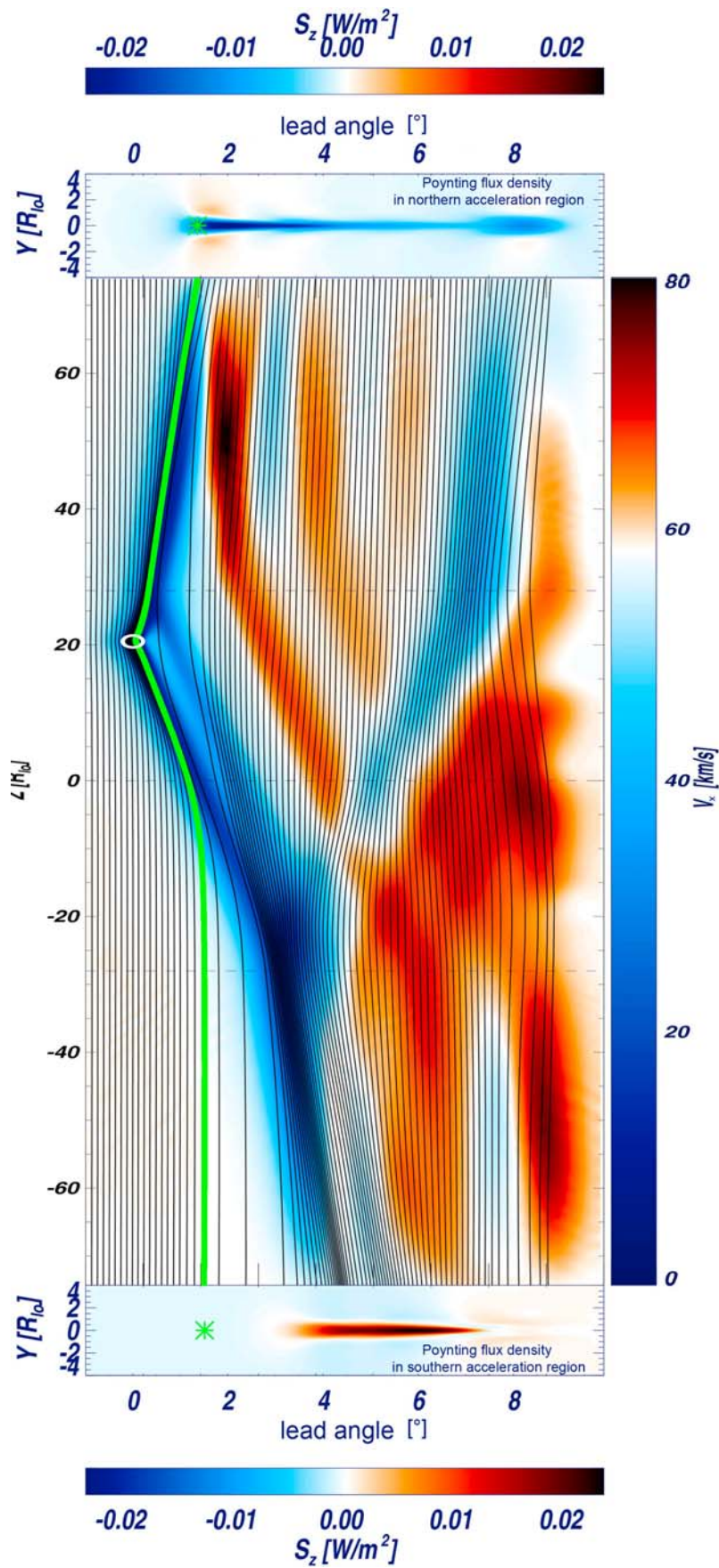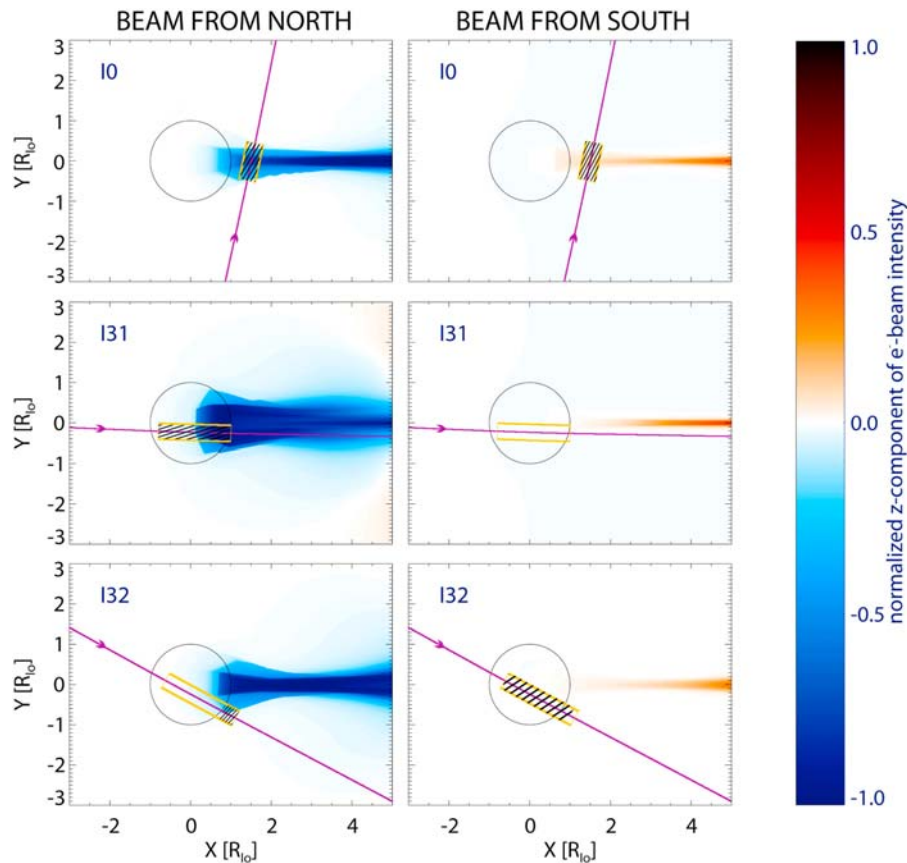
Figure 3

Figure 4. Color-coded: Simulated electron beam intensity in Galileo's orbital plane for different flyby scenarios. Galileo trajectory plotted in magenta (I0, wake flyby in equatorial plane; I31, north polar flyby; I32, south polar flyby). The yellow squares depict observed field-aligned electron beam locations [*Williams and Thorne*, 2003]. (left) Beams generated in the northern hemisphere. Hatched area depicts observed beam from the north. (right) Beams generated in the southern hemisphere. Hatched area depicts observed beam from the south.

data shows some evidence for an unusually strong interaction for Io's position high above the centrifugal equator. The magnetic field perturbation in x direction δB_x of ~900 nT at a background field strength of ~1950 nT [*Xin et al.* 2006, Figure 4] is considerably higher than what we simulate with our far-field model. With such a strong perturbation our simulated southern beam would be shifted upstream and show better agreement with the observations.

5. Conclusions

[26] The method described in this paper, although including a few simplifications demonstrates that equatorial electron beams are located downstream from the initial

Alfvén wave generator depending on the ratio of two crucial parameters: Alfvénic travel time and convection time. Our model predicts that the electron beams are detached downstream instead of being close or connected to the satellite if the sub-Alfvénic interaction is weaker. For Io as a known Alfvén wave generator both important parameters vary and in situ measurements are available. Thus it represents a good prime example for our studies. Our results support the idea that equatorial field-aligned electron beams measured on three Galileo flybys originate from the acceleration region above the Jovian ionosphere. Our simulated beam topology qualitatively agrees with the Galileo observations to a large extent. We trace the beams to the opposite hemisphere in our simulations and obtain estimates for a leading spot offset

Figure 3. Shown are x-y planes above the (top) northern and (bottom) southern Jovian ionosphere. The color code marks the z component of the Poynting flux density which reaches the northern and southern Jovian acceleration regions, respectively. X coordinates give the longitudinal offset with respect to Io's magnetic longitude, the so-called lead angle. (middle) Magnetic field lines plotted over color-coded x component of the plasma bulk velocity $\mathbf{v}_x$, with blue color for decelerated and red for accelerated plasma with respect to the background velocity (white). The thick green field line is the travel path of an electron beam originating in the acceleration region above Jupiter's ionosphere and depicted with the star symbol in Figure 3 (top). The star symbol in Figure 3 (bottom) is the simulated position of the beam, when it finally reaches the southern ionosphere.

which agree with observational data by *Bonfond et al.* [2008]. Other moons like Ganymede, Europa and Enceladus exhibit similar interaction with the planetary magnetosphere and are therefore likely to display comparable beam phenomena. At Callisto there is evidence for electron beams during the C3 encounter at some distance downstream the moon [*Mauk and Saur*, 2007]. The shape and location of these beams can be used to constrain Callisto's interaction with Jupiter's magnetosphere. When the interaction is weaker than at Io, or the Alfvén travel time larger, then the beams might be detached from the satellite. Observational searches for these beams at other satellites thus need to be extended to the downstream region.

References

Acuña, M. H., F. M. Neubauer, and N. F. Ness (1981), Standing Alfven wave current system at Io: Voyager 1 observations, *J. Geophys. Res.*, *86*(A10), 8513–8521, doi:10.1029/JA086iA10p08513.

Bagenal, F. (1983), Alfven wave propagation in the Io plasma torus, *J. Geophys. Res.*, *88*(A4), 3013–3025, doi:10.1029/JA088iA04p03013.

Bagenal, F., and J. D. Sullivan (1981), Direct plasma measurements in the Io torus and inner magnetosphere of Jupiter, *J. Geophys. Res.*, *86*(A10), 8447–8466, doi:10.1029/JA086iA10p08447.

Bonfond, B., D. Grodent, J.-C. Gérard, A. Radioti, J. Saur, and S. Jacobsen (2008), UV Io footprint leading spot: A key feature for understanding the UV Io footprint multiplicity?, *Geophys. Res. Lett.*, *35*, L05107, doi:10.1029/2007GL032418.

Bonfond, B., D. Grodent, J.-C. Gérard, A. Radioti, V. Dols, P. A. Delamere, and J. T. Clarke (2009), The Io UV footprint: Location, interspot distances and tail vertical extent, *J. Geophys. Res.*, *114*, A07224, doi:10.1029/2009JA014312.

Carlson, C. W., et al. (1998), FAST observations in the downward auroral current region: Energetic upgoing electron beams, parallel potential drops, and ion heating, *Geophys. Res. Lett.*, *25*(12), 2017–2020, doi:10.1029/98GL00851.

Chust, T., A. Roux, W. S. Kurth, D. A. Gurnett, M. G. Kivelson, and K. K. Khurana (2005), Are Io's Alfvén wings filamented? Galileo observations, *Planet. Space Sci.*, *53*, 395–412, doi:10.1016/j.pss.2004.09.021.

Clarke, J. T., et al. (1996), Far-ultraviolet imaging of Jupiter's aurora and the Io "footprint," *Science*, *274*, 404–409, doi:10.1126/science.274.5286.404.

Connerney, J. E. P., R. Baron, T. Satoh, and T. Owen (1993), Images of excited H_3^+ at the foot of the Io flux tube in Jupiter's atmosphere, *Science*, *262*, 1035–1038, doi:10.1126/science.262.5136.1035.

Crary, F. J. (1997), On the generation of an electron beam by Io, *J. Geophys. Res.*, *102*(A1), 37–50, doi:10.1029/96JA02409.

Dols, V., J. C. Gérard, J. T. Clarke, J. Gustin, and D. Grodent (2000), Diagnostics of the Jovian aurora deduced from ultraviolet spectroscopy: Model and HST/GHRS observations, *Icarus*, *147*, 251–266, doi:10.1006/icar.2000.6415.

Dols, V., P. A. Delamere, and F. Bagenal (2008), A multispecies chemistry model of Io's local interaction with the plasma torus, *J. Geophys. Res.*, *113*, A09208, doi:10.1029/2007JA012805.

Drell, S. D., H. M. Foley, and M. A. Ruderman (1965), Drag and propulsion of large satellites in the ionosphere: An Alfvén propulsion engine in space, *J. Geophys. Res.*, *70*(13), 3131–3145, doi:10.1029/JZ070i013p03131.

Frank, L. A., and W. R. Paterson (1999), Intense electron beams observed at Io with the Galileo spacecraft, *J. Geophys. Res.*, *104*(A12), 28,657–28,670, doi:10.1029/1999JA900402.

Frank, L. A., and W. R. Paterson (2002a), Galileo observations of electron beams and thermal ions in Jupiter's magnetosphere and their relationship to the auroras, *J. Geophys. Res.*, *107*(A12), 1478, doi:10.1029/2001JA009150.

Frank, L. A., and W. R. Paterson (2002b), Plasmas observed with the Galileo spacecraft during its flyby over Io's northern polar region, *J. Geophys. Res.*, *107*(A8), 1220, doi:10.1029/2002JA009240.

Gérard, J.-C., A. Saglam, D. Grodent, and J. T. Clarke (2006), Morphology of the ultraviolet Io footprint emission and its control by Io's location, *J. Geophys. Res.*, *111*, A04202, doi:10.1029/2005JA011327.

Goldreich, P., and D. Lynden-Bell (1969), Io, a Jovian unipolar inductor, *Astrophys. J.*, *156*, 59–78, doi:10.1086/149947.

Hess, S., F. Mottez, and P. Zarka (2007), Jovian S burst generation by Alfvén waves, *J. Geophys. Res.*, *112*, A11212, doi:10.1029/2006JA012191.

Jacobsen, S., F. M. Neubauer, J. Saur, and N. Schilling (2007), Io's nonlinear MHD-wave field in the heterogeneous Jovian magnetosphere, *Geophys. Res. Lett.*, *34*, L10202, doi:10.1029/2006GL029187.

Jones, S. T., and Y.-J. Su (2008), Role of dispersive Alfvén waves in generating parallel electric fields along the Io-Jupiter fluxtube, *J. Geophys. Res.*, *113*, A12205, doi:10.1029/2008JA013512.

Klumpar, D. M. (1990), Near equatorial signatures of dynamic auroral processes, in *Physics of Space Plasmas*, pp. 265–276, Scientific, Cambridge, Mass.

Klumpar, D. M., J. M. Quinn, and E. G. Shelley (1988), Counter-streaming electrons at the geomagnetic equator near 9 Earth radii, *Geophys. Res. Lett.*, *15*, 1295–1298, doi:10.1029/GL015i011p01295.

Knight, S. (1973), Parallel electric fields, *Planet. Space Sci.*, *21*, 741–750, doi:10.1016/0032-0633(73)90093-7.

Mauk, B. H., and J. Saur (2007), Equatorial electron beams and auroral structuring at Jupiter, *J. Geophys. Res.*, *112*, A10221, doi:10.1029/2007JA012370.

Mauk, B. H., D. J. Williams, R. W. McEntire, K. K. Khurana, and J. G. Roederer (1999), Storm-like dynamics of Jupiter's inner and middle magnetosphere, *J. Geophys. Res.*, *104*(A10), 22,759–22,778, doi:10.1029/1999JA900097.

Mauk, B. H., D. J. Williams, and A. Eviatar (2001), Understanding Io's space environment interaction: Recent energetic electron measurements from Galileo, *J. Geophys. Res.*, *106*(A11), 26,195–26,208, doi:10.1029/2000JA002508.

Mauk, B. H., B. J. Anderson, and R. M. Thorne (2002), Magnetosphere-ionosphere coupling at Earth, Jupiter, and beyond, in *Atmospheres in the Solar System: Comparative Aeronomy*, *Geophys. Monogr. Ser.*, vol. 130, edited by M. Mendillo, A. Nagy, and J. H. Waite, pp. 97–114, AGU, Washington, D. C.

Mitchell, D. G., et al. (2009), Ion conics and electron beams associated with auroral processes on Saturn, *J. Geophys. Res.*, *114*, A02212, doi:10.1029/2008JA013621.

Moncuquet, M., F. Bagenal, and N. Meyer-Vernet (2002), Latitudinal structure of outer Io plasma torus, *J. Geophys. Res.*, *107*(A9), 1260, doi:10.1029/2001JA900124.

Neubauer, F. M. (1980), Nonlinear standing Alfven wave current system at Io: Theory, *J. Geophys. Res.*, *85*(A3), 1171–1178, doi:10.1029/JA085iA03p01171.

Neubauer, F. M. (1998), The sub-Alfvénic interaction of the Galilean satellites with the Jovian magnetosphere, *J. Geophys. Res.*, *103*(E9), 19,843–19,866, doi:10.1029/97JE03370.

Prangé, R., D. Rego, D. Southwood, P. Zarka, S. Miller, and W. Ip (1996), Rapid energy dissipation and variability of the Io-Jupiter electrodynamic circuit, *Nature*, *379*, 323–325, doi:10.1038/379323a0.

Saur, J. (2004), A model of Io's local electric field for a combined Alfvénic and unipolar inductor far-field coupling, *J. Geophys. Res.*, *109*, A01210, doi:10.1029/2002JA009354.

Saur, J., F. M. Neubauer, D. F. Strobel, and M. E. Summers (1999), Three-dimensional plasma simulation of Io's interaction with the Io plasma torus: Asymmetric plasma flow, *J. Geophys. Res.*, *104*(A11), 25,105–25,126, doi:10.1029/1999JA900304.

Saur, J., F. M. Neubauer, D. F. Strobel, and M. E. Summers (2002), Interpretation of Galileo's Io plasma and field observations: I0, I24, and I27 flybys and close polar passes, *J. Geophys. Res.*, *107*(A12), 1422, doi:10.1029/2001JA005067.

Saur, J., F. M. Neubauer, J. E. P. Connerney, P. Zarka, and M. G. Kivelson (2004), Plasma interaction of Io with its plasma torus, in *Jupiter: The Planet, Satellites and Magnetosphere*, *Cambridge Planet. Sci.*, vol. 1, edited by F. Bagenal, T. E. Dowling, and W. B. McKinnon, pp. 537–560, Cambridge Univ. Press, Cambridge, U. K.

Saur, J., et al. (2006), Anti-planetward auroral electron beams at Saturn, *Nature*, *439*, 699–702, doi:10.1038/nature04401.

Smith, R. A., and C. K. Goertz (1978), On the modulation of the Jovian decametric radiation by Io: 1. Acceleration of charged particles, *J. Geophys. Res.*, *83*(A6), 2617–2627, doi:10.1029/JA083iA06p02617.

Stone, J. M., and M. L. Norman (1992), ZEUS-2D: A radiation magnetohydrodynamics code for astrophysical flows in two space dimensions. I — The hydrodynamic algorithms and tests., *Astrophys. J. Suppl. Ser.*, *80*, 753–790, doi:10.1086/191680.

Su, Y.-J., R. E. Ergun, F. Bagenal, and P. A. Delamere (2003), Io-related Jovian auroral arcs: Modeling parallel electric fields, *J. Geophys. Res.*, *108*(A2), 1094, doi:10.1029/2002JA009247.

Swift, D. W. (2007), Simulation of auroral electron acceleration by inertial Alfvén waves, *J. Geophys. Res.*, *112*, A12207, doi:10.1029/2007JA012423.

Tomás, A. T., J. Woch, N. Krupp, A. Lagg, K.-H. Glassmeier, and W. S. Kurth (2004), Energetic electrons in the inner part of the Jovian magnetosphere and their relation to auroral emissions, *J. Geophys. Res.*, *109*, A06203, doi:10.1029/2004JA010405.

Williams, D. J., and R. M. Thorne (2003), Energetic particles over Io's polar caps, *J. Geophys. Res.*, *108*(A11), 1397, doi:10.1029/2003JA009980.

Williams, D. J., et al. (1996), Electron beams and ion composition measured at Io and in its torus, *Science*, *274*, 401–403, doi:10.1126/science.274.5286.401.

Williams, D. J., R. M. Thorne, and B. Mauk (1999), Energetic electron beams and trapped electrons at Io, *J. Geophys. Res.*, *104*(A7), 14,739–14,754, doi:10.1029/1999JA900115.

Wright, A. N. (1987), The interaction of Io's Alfven waves with the Jovian magnetosphere, *J. Geophys. Res.*, *92*(A9), 9963–9970, doi:10.1029/JA092iA09p09963.

Xin, L., D. A. Gurnett, and M. G. Kivelson (2006), Whistler mode auroral hiss emissions observed near Jupiter's moon Io, *J. Geophys. Res.*, *111*, A04212, doi:10.1029/2005JA011411.

Zarka, P. (1998), Auroral radio emissions at the outer planets: Observations and theories, *J. Geophys. Res.*, *103*, 20,159–20,194, doi:10.1029/98JE01323.

B. Bonfond, J.-C. Gérard, and D. Grodent, Laboratory for Planetary and Atmospheric Physics, Université de Liège, B-4000 Liège, Belgium.

S. Jacobsen, F. M. Neubauer, and J. Saur, Institut für Geophysik und Meteorologie, Universität zu Köln, Albertus-Magnus-Platz, D-50923 Cologne, Germany. (jacobsen@geo.uni-koeln.de)